

# Electron impact ionization of the $\text{SiD}_x$ ( $x=1-3$ ) free radicals

V. Tarnovsky

*Physics Department, City College of C.U.N.Y., New York*

H. Deutsch

*Fachbereich Physik, Universität Greifswald, Germany*

K. Becker

*Physics Department, City College of C.U.N.Y., New York*

(Received 24 May 1996; accepted 9 July 1996)

We report measurements of absolute cross sections for the electron-impact ionization and dissociative ionization of the  $\text{SiD}_x$  ( $x=1-3$ ) free radicals from threshold to 200 eV using the fast-neutral-beam technique. The deuterated rather than the protonated target species were used in order to allow a better separation of the various product ions from a given parent in our apparatus. A common feature of all three radicals studied in this work is a dominant parent ionization cross section with essentially the same absolute value of roughly  $3.7 \times 10^{-16} \text{ cm}^2$  at 70 eV. Dissociative ionization processes for all three targets are less significant with a single dissociative process dominating in each case, viz. the removal of a single D atom ( $\text{SiD}_x + e^- \rightarrow \text{SiD}_{x-1}^+ + \text{D} + 2e^-$ ). The cross section for this dominant dissociative ionization channel also had the same maximum value of about  $1.2 \times 10^{-16} \text{ cm}^2$  for all three targets. A comparison of the experimentally determined total single ionization cross sections with calculated cross sections using a modified additivity rule showed good to satisfactory agreement for all three targets in terms of the absolute values, but reveals some discrepancies in the cross section shapes. © 1996 American Institute of Physics. [S0021-9606(96)00539-9]

## I. INTRODUCTION

Silane,  $\text{SiH}_4$ , is a frequently used constituent of low-temperature processing plasmas used in the fabrication of microelectronic devices and other semiconducting components.  $\text{SiH}_4$  plays a particularly important role in the plasma-assisted deposition of silicon and amorphous silicon-hydride ( $a\text{:SiH}$ ) films.<sup>1</sup> Silane is also a constituent of the atmosphere of the planet Saturn as well as a minor constituent of the atmospheres of several other planets and their satellites. In both environments, dissociation of  $\text{SiH}_4$  by collisional interaction and/or photodissociation results in the formation of the free radicals  $\text{SiH}_3$ ,  $\text{SiH}_2$ , and  $\text{SiH}$ . Cross sections for the production of the various parent and fragment ions by electron collisional ionization and dissociative ionization of  $\text{SiH}_x$  ( $x=1-4$ ) are important for the understanding, the modeling, and the characterization of the relevant process chemistry in technological discharge plasmas and also in planetary atmospheres.<sup>1-3</sup> There have been several measurements of the electron-impact ionization and dissociative ionization of the parent  $\text{SiH}_4$  molecule.<sup>4-7</sup> The results of these measurements fall into two categories. The early work of Saalfeld and Svec<sup>4</sup> and the more recent Fourier transform mass spectrometer (FTMS) study of Haaland<sup>5</sup> reported small partial ionization cross sections for all product ions with peak cross section values in the  $10^{-17} \text{ cm}^2$  range. On the other hand, two experiments using different types of quadrupole mass spectrometers<sup>6,7</sup> yielded partial ionization cross sections which were higher by as much as a factor of 5. However, there were also significant discrepancies between these two measurements in terms of the absolute cross-section values

as well as in the reported cross-section shapes. This troubling uncertainty in the ionization cross section data of a technologically relevant molecule such as silane motivated another study of the  $\text{SiH}_4$  ionization using a well-established high resolution double-focusing mass spectrometer.<sup>8</sup> No data have been reported so far regarding the ionization and dissociative ionization of the  $\text{SiH}_x$  ( $x=1-3$ ) free radicals by electron impact. The only ionization cross-section measurements involving Si-bearing species are those of Freund and co-workers for the  $\text{SiF}_x$  ( $x=1-3$ ) radicals.<sup>9-11</sup>

This paper reports absolute partial cross sections for the electron-impact ionization and dissociative ionization of the  $\text{SiD}_x$  ( $x=1-3$ ) free radicals from threshold to 200 eV. We used the deuterated rather than the protonated target species as was done in our previous studies of  $\text{CD}_x$  ( $x=1-4$ ) to facilitate a better separation of the various product ions from a given parent<sup>12</sup> (ionization cross sections are insensitive to isotope effects<sup>13-15</sup>). For each target, the total single ionization cross section was estimated from the measured partial ionization cross sections. A comparison with calculated total single ionization cross sections based on a modified additivity rule<sup>16</sup> showed good to satisfactory agreement for all three targets.

## II. EXPERIMENT

Previous publications have given detailed descriptions of the fast-beam apparatus and of the experimental procedure employed in the determination of absolute partial ionization cross sections.<sup>17-20</sup> A dc discharge biased at typically 2–3 kV through  $\text{SiD}_4$  served as the primary ion source. The pri-

mary ions are mass selected in a Wien filter and sent through a charge-transfer cell filled with Xe where a fraction of the ions is neutralized by near-resonant charge transfer. Xe with an ionization energy of 12.14 eV<sup>21</sup> was found to be an appropriate charge neutralization target for all three  $\text{SiD}_x$  ( $x = 1-3$ ) radicals whose ionization energies are in the range 8–9 eV.<sup>21–23</sup> Similar to what was observed in previous studies,<sup>18,20,24–26</sup> efficient charge transfer was not critically dependent on an exact match of the ionization energies of the charge-transfer partners. The residual ions were removed from the target gas beam by electrostatic deflection and most species in Rydberg states were quenched in a region of high electric field. The neutral beam was subsequently crossed at right angles by a well-characterized electron beam (5–200 eV beam energy, 0.5 eV FWHM energy spread, 0.03–0.4 mA beam current). The product ions were focused in the entrance plane of an electrostatic hemispherical analyzer which separates ions of different charge-to-mass ratios (i.e., parent ions from fragment ions). The ions leaving the analyzer were detected by a channel electron multiplier (CEM). The well-established Kr or Ar absolute ionization cross sections served as a convenient normalization standard to put the relative cross-section functions on an absolute scale.<sup>18–20</sup> This was done by using the Kr or Ar benchmark cross sections to calibrate the pyroelectric crystal. The calibrated detector, in turn, is then used to determine the flux of the neutral target beam in absolute terms. This procedure avoids the frequent and prolonged exposure of the sensitive pyroelectric crystal to fairly intense ion beams.<sup>17,18</sup>

We established for each target that all fragment ions (except for  $\text{D}^+$ , see discussion below) with an excess kinetic energy of less than 2–2.5 eV per fragment ion are collected and detected with 100% efficiency using a combination of *in situ* experimental studies and ion trajectory modelling calculations.<sup>23</sup> Furthermore, careful threshold studies revealed little evidence of the presence of excited target species (vibrationally excited species, metastables, and species in high-lying Rydberg states) in the incident neutral beams for  $\text{SiD}_3$ ,  $\text{SiD}_2$ , and  $\text{SiD}$ . In addition to these experimental checks, which are necessary for any target studied using the fast-beam technique in order to ensure that the measured cross sections are free from systematic uncertainties to the maximum extent possible,<sup>19,20,24</sup> we also carried out all experimental checks pertaining specifically to hydrogen- and deuterium-containing targets as described in detail in Ref. 12.

We found little evidence of the presence of  $\text{D}^+$  fragment ions from the dissociative ionization of all three  $\text{SiD}_x$  targets. On the other hand, ion trajectory modeling calculations suggest significant losses of  $\text{D}^+$  fragment ion from  $\text{SiD}_x$  for excess kinetic energies as low as 0.5 eV per fragment ion. This renders it difficult, if not impossible, to determine reliable absolute partial  $\text{D}^+$  ionization cross sections for any of the three  $\text{SiD}_x$  targets using our experimental approach. Therefore, no quantitative data for  $\text{D}^+$  formation from any of the  $\text{SiD}_x$  target species ( $x = 1-3$ ) are reported in this paper.

It was difficult to establish the optimum operating conditions for the dc Colutron discharge using  $\text{SiD}_4$  as the feed

gas and it was equally difficult to maintain a stable discharge performance for more than a few hours at a time. For instance, the ratio of  $\text{SiD}_3^+:\text{SiD}_2^+:\text{SiD}^+$  primary ions extracted from the discharge varied greatly from day to day and was found to depend not only on the discharge parameters, but also critically on the “history” of the discharge vessel and crucially on the temperature in the ion source. New, clean ion sources tended to perform less reliably than ion sources which had been passivated by extended prior exposure to a  $\text{SiD}_4$  discharge.

### III. RESULTS AND DISCUSSION

For each of the three targets, we first measured the relative partial parent ionization cross section from threshold to 200 eV followed by a measurement of the relative partial cross sections for the corresponding fragment ions. All measurements followed the previously described experimental procedure.<sup>12,18,20,24</sup> In all cases studied here, the measurements were limited to singly charged ions, since cross sections for the formation of doubly charged ions were found to be at or below the detection sensitivity of our apparatus (peak cross sections below  $0.05 \times 10^{-16} \text{ cm}^2$ ). The parent ionization cross-section sections were then put on an absolute scale by normalization to the well-known Kr or Ar benchmark cross sections as discussed before. All dissociative ionization cross sections were subsequently normalized to the parent ionization cross section for a given target. In all cases, careful threshold studies were carried out to check for the presence of excited species in the incident neutral beam and to determine the appearance energies for the various product ions. This is particularly crucial for dissociative ionization processes, since the appearance energy when compared to thermochemical and spectroscopic data for the formation of a particular fragment ion provides information about the (minimum) excess kinetic energy with which the fragment ion is formed.

The absolute cross sections were determined with uncertainties of  $\pm 15\%$  for the parent ionization cross sections and  $\pm 18\%$  for the dissociative ionization cross sections. These error margins, which are similar to what we quoted previously for ionization cross sections measured for other free radicals in the same apparatus,<sup>12,18,20,24</sup> include statistical uncertainties and all known sources of systematic uncertainties.

#### A. Measured partial ionization cross sections for the $\text{SiD}_x$ ( $x = 1-3$ ) free radicals

Figure 1 shows the absolute cross sections for the formation of  $\text{SiD}_3^+$  and  $\text{SiD}_2^+$  ions from the  $\text{SiD}_3$  free radical from threshold to 200 eV. Both curves represent the result of a single data run. The peak cross sections for the formation of  $\text{SiD}^+$  fragment ions from  $\text{SiD}_3$  was found to be less than  $0.1 \times 10^{-16} \text{ cm}^2$ . Cross sections for the other singly charged fragment ions ( $\text{D}^+$ ,  $\text{Si}^+$ ) and cross sections for multiply charged ions were even smaller. We find cross sections at 70 eV of  $3.68 \pm 0.50 \times 10^{-16} \text{ cm}^2$  ( $\text{SiD}_3^+$ ) and  $1.13 \pm 0.21 \times 10^{-16} \text{ cm}^2$  ( $\text{SiD}_2^+$ ). The cross-section values are also listed in Table I for easier reference. Note, that the cross-section values in

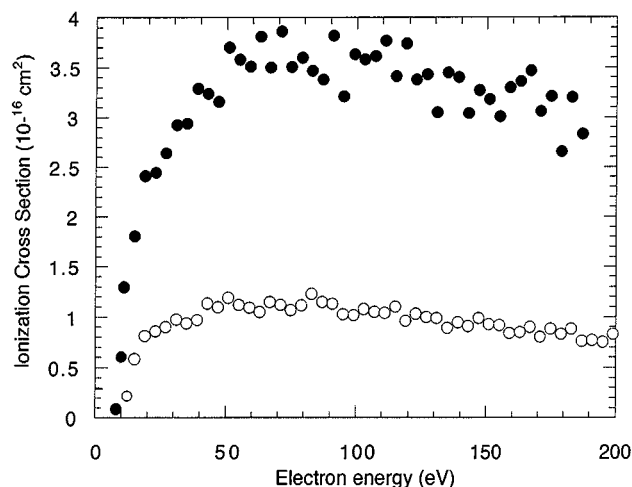


FIG. 1. Absolute cross sections for the formation of the SiD<sub>3</sub><sup>+</sup> parent ions (●) and the SiD<sub>2</sub><sup>+</sup> (○) fragment ions from SiD<sub>3</sub> as a function of electron energy.

Table I represent the average of several individual data runs. The cross section tables (with particular emphasis on the low energy regime) are presented primarily for the convenience of practitioners who use these cross-section data for modeling purposes or other applications (e.g., in the quantitative analysis of threshold ionization mass spectroscopic studies for plasma diagnostics purposes, see Ref. 27). The measured appearance energy of the SiD<sub>3</sub><sup>+</sup> parent ion of  $8.0 \pm 0.5$  eV is very close to the known 8.14 eV ionization energy of SiD<sub>3</sub> in its vibrational ground state.<sup>21–23</sup> The near-threshold region of the SiD<sub>3</sub><sup>+</sup> cross section is shown in Fig. 2. We found no evidence of an extended curvature in the near-threshold region or of a significant shift of the measured appearance energy to lower values. This indicates that the vibrational excitation of the SiD<sub>3</sub> radicals in the target beam is negligible and that there is no appreciable contamination of the target beam due to the presence of metastable SiD<sub>3</sub> radicals or SiD<sub>3</sub> radicals in long-lived Rydberg states. The measured appearance energy of the SiD<sub>2</sub><sup>+</sup> fragment ions from SiD<sub>3</sub> of  $11.3 \pm 0.7$  eV is only marginally higher than the thermochemical minimum energy required for the formation of this fragment ion.<sup>21–23</sup> This indicates that the SiD<sub>2</sub><sup>+</sup> fragment ions are formed with little excess kinetic energy.

Figure 3 shows the absolute cross sections for the formation of SiD<sub>2</sub><sup>+</sup> and SiD<sup>+</sup> ions from the SiD<sub>2</sub> free radical from threshold to 200 eV. Note, that these curves represent the average of several data runs. The peak cross sections for the formation of other singly charged fragment ions (D<sup>+</sup>, Si<sup>+</sup>) and the cross sections for multiply charged ions were found to be less than  $0.1 \times 10^{-16}$  cm<sup>2</sup> each. We find cross sections at 70 eV of  $3.75 \pm 0.55 \times 10^{-16}$  cm<sup>2</sup> (SiD<sub>2</sub><sup>+</sup>) and  $1.27 \pm 0.23 \times 10^{-16}$  cm<sup>2</sup> (SiD<sup>+</sup>). Table II presents our measured SiD<sub>2</sub> ionization cross-sections data in tabulated form for convenient quantitative reference. The measured appearance energies of the SiD<sub>2</sub><sup>+</sup> parent ions of  $8.5 \pm 0.5$  eV is close to the known SiD<sub>2</sub> ionization energy of 8.92 eV in its vibrational ground state. Threshold studies revealed little evidence

TABLE I. Absolute cross sections for the formation of SiD<sub>3</sub><sup>+</sup> and SiD<sub>2</sub><sup>+</sup> ions from SiD<sub>3</sub> by electron impact. The cross sections are given in units of  $10^{-16}$  cm<sup>2</sup>.

| Electron energy<br>(eV) | Ionization cross section (in $10^{-16}$ cm <sup>2</sup> ) |   |
|-------------------------|---|---|
|                         | SiD <sub>3</sub> <sup>+</sup> /SiD <sub>3</sub>           | SiD <sub>2</sub> <sup>+</sup> /SiD <sub>3</sub> |
| 8.0                     | 0.01  |   |
| 8.5                     | 0.04  |   |
| 9.0                     | 0.08  |   |
| 9.5                     | 0.16  |   |
| 10.0                    | 0.24  |   |
| 11.0                    | 0.36  |   |
| 12.0                    | 0.47  | 0.04  |
| 13.0                    | 0.66  | 0.10  |
| 14.0                    | 0.77  | 0.16  |
| 15.0                    | 0.88  | 0.22  |
| 16.0                    | 0.98  | 0.27  |
| 17.0                    | 1.08  | 0.33  |
| 18.0                    | 1.20  | 0.39  |
| 19.0                    | 1.32  | 0.46  |
| 20.0                    | 1.43  | 0.51  |
| 22.0                    | 1.64  | 0.59  |
| 24.0                    | 1.89  | 0.67  |
| 26.0                    | 2.18  | 0.75  |
| 28.0                    | 2.45  | 0.83  |
| 30.0                    | 2.68  | 0.93  |
| 35.0                    | 2.92  | 0.97  |
| 40.0                    | 3.15  | 1.01  |
| 45.0                    | 3.30  | 1.06  |
| 50.0                    | 3.44  | 1.09  |
| 60.0                    | 3.60  | 1.11  |
| 70.0                    | 3.68  | 1.13  |
| 80.0                    | 3.65  | 1.13  |
| 90.0                    | 3.63  | 1.12  |
| 100.0                   | 3.59  | 1.09  |
| 120.0                   | 3.48  | 1.01  |
| 140.0                   | 3.29  | 0.95  |
| 160.0                   | 3.15  | 0.88  |
| 180.0                   | 2.93  | 0.83  |
| 200.0                   | 2.66  | 0.77  |

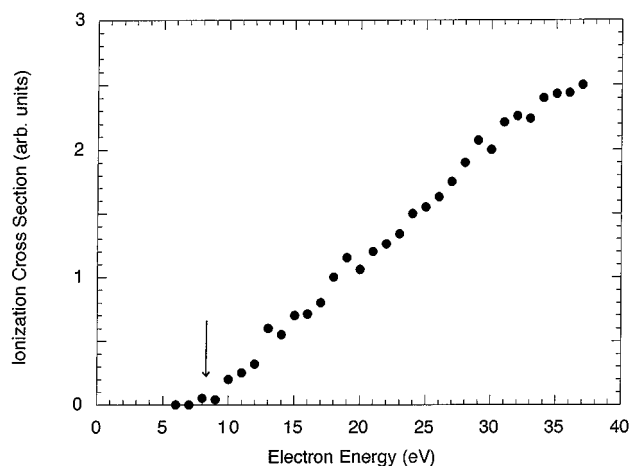


FIG. 2. Near-threshold region of the SiD<sub>3</sub><sup>+</sup> partial ionization cross section. The ionization energy of SiD<sub>3</sub> in its vibrational ground state is indicated by an arrow. (See text for further details.)

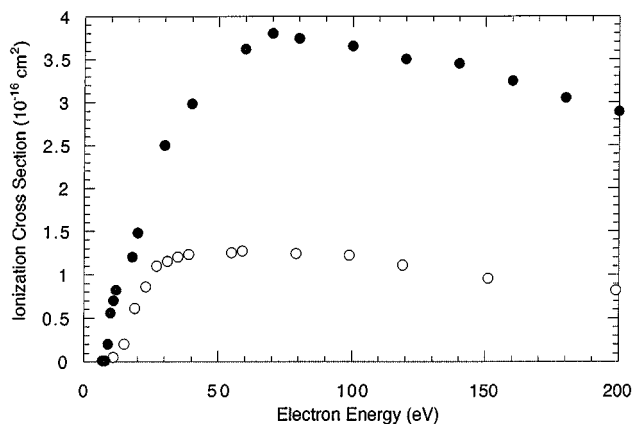


FIG. 3. Absolute cross sections for the formation of the SiD<sub>2</sub><sup>+</sup> parent ions (●) and the SiD<sup>+</sup> (○) fragment ions from SiD<sub>2</sub> as a function of electron energy.

of an extended curvature in the near-threshold region or of a shift of the measured appearance energy to a value signifi-

TABLE II. Absolute cross sections for the formation of SiD<sub>2</sub><sup>+</sup> and SiD<sup>+</sup> ions from SiD<sub>2</sub> by electron impact. The cross sections are given in units of 10<sup>-16</sup> cm<sup>2</sup>.

| Electron energy<br>(eV) | Ionization cross section (in 10 <sup>-16</sup> cm <sup>2</sup> ) |                                    |
|-------------------------|--|------------------------------------|
|                         | SiD <sub>2</sub> <sup>+</sup> /SiD <sub>2</sub>                  | SiD <sup>+</sup> /SiD <sub>2</sub> |
| 8.5                     | 0.01   |                                    |
| 9.0                     | 0.08   |                                    |
| 9.5                     | 0.16   |                                    |
| 10.0                    | 0.24   |                                    |
| 11.0                    | 0.40   |                                    |
| 12.0                    | 0.58   |                                    |
| 13.0                    | 0.74   | 0.04                               |
| 14.0                    | 0.91   | 0.12                               |
| 15.0                    | 1.03   | 0.20                               |
| 16.0                    | 1.12   | 0.25                               |
| 17.0                    | 1.22   | 0.32                               |
| 18.0                    | 1.31   | 0.40                               |
| 19.0                    | 1.41   | 0.46                               |
| 20.0                    | 1.50   | 0.53                               |
| 22.0                    | 1.68   | 0.65                               |
| 24.0                    | 1.90   | 0.78                               |
| 26.0                    | 2.15   | 0.90                               |
| 28.0                    | 2.39   | 0.98                               |
| 30.0                    | 2.59   | 1.02                               |
| 35.0                    | 2.74   | 1.07                               |
| 40.0                    | 2.95   | 1.12                               |
| 45.0                    | 3.14   | 1.16                               |
| 50.0                    | 3.31   | 1.19                               |
| 60.0                    | 3.63   | 1.23                               |
| 70.0                    | 3.75   | 1.27                               |
| 80.0                    | 3.74   | 1.26                               |
| 90.0                    | 3.72   | 1.23                               |
| 100.0                   | 3.66   | 1.20                               |
| 120.0                   | 3.47   | 1.10                               |
| 140.0                   | 3.23   | 1.01                               |
| 160.0                   | 3.12   | 0.92                               |
| 180.0                   | 2.91   | 0.86                               |
| 200.0                   | 2.65   | 0.78                               |

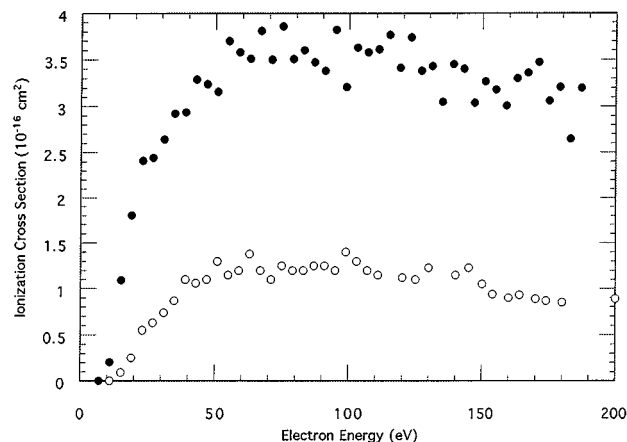


FIG. 4. Absolute cross sections for the formation of the SiD<sup>+</sup> parent ions (●) and the Si<sup>+</sup> (○) fragment ions from SiD as a function of electron energy.

cantly lower than the known ionization energy. This indicates that the vibrational excitation of the SiD<sub>2</sub> radicals in the target beam is negligible and that there is no appreciable contamination of the target beam due to the presence of metastable SiD<sub>2</sub> radicals or SiD<sub>2</sub> radicals in long-lived Rydberg states similar to what was observed in the case of SiD<sub>3</sub>. The measured appearance energy of the SiD<sup>+</sup> fragment ions from SiD<sub>2</sub> of 12.2±0.7 eV is higher than the thermochemical minimum energy required for the formation of this fragment ion by less than 1 eV assuming a Si–D bond dissociation energy of about 3 eV.<sup>21–23,28,29</sup> This indicates that the SiD<sup>+</sup> fragment ions are formed with little excess kinetic energy.

Figure 4 shows the absolute cross sections for the formation of SiD<sup>+</sup> and Si<sup>+</sup> ions from the SiD free radical from threshold to 200 eV. The two data sets represent individual data runs. The peak cross sections for the formation of D<sup>+</sup> fragment ions was found to be less than 0.1×10<sup>-16</sup> cm<sup>2</sup>. Cross sections for multiply charged ions were even smaller. We find cross sections at 70 eV of 3.70±0.55×10<sup>-16</sup> cm<sup>2</sup> (SiD<sup>+</sup>) and 1.25±0.22×10<sup>-16</sup> cm<sup>2</sup> (Si<sup>+</sup>). Table III presents the measured SiD partial ionization cross sections averaged over several individual data runs in tabulated form for convenient quantitative reference. The measured appearance energies of the SiD<sup>+</sup> parent ions of 7.6±0.5 eV is close to the well-known ionization of 7.89 eV of SiD in its vibrational ground state. We found little evidence of an extended curvature in the near-threshold region or of a significant shift of the measured appearance energy to lower values. This indicates that the vibrational excitation of the SiD radicals in the target beam is negligible and that there is no appreciable contamination of the target beam due to the presence of metastable SiD radicals or SiD radicals in long-lived Rydberg states similar to what was observed in the case of SiD<sub>3</sub>. The measured appearance energy of the Si<sup>+</sup> fragment ions from SiD of 11.3±0.7 eV is higher than the thermochemical minimum energy required for the formation of this fragment ion by less than 1 eV.<sup>21–23</sup> This indicates that the Si<sup>+</sup> fragment ions are formed with little excess kinetic energy.

TABLE III. Absolute cross sections for the formation of SiD<sup>+</sup> and Si<sup>+</sup> ions from SiD by electron impact. The cross sections are given in units of 10<sup>-16</sup> cm<sup>2</sup>.

| Electron energy<br>(eV) | Ionization cross section (in 10 <sup>-16</sup> cm <sup>2</sup> ) |                      |
|-------------------------|--|----------------------|
|                         | SiD <sup>+</sup> /SiD  | Si <sup>+</sup> /SiD |
| 8.0                     | 0.08   |                      |
| 8.5                     | 0.18   |                      |
| 9.0                     | 0.28   |                      |
| 9.5                     | 0.40   |                      |
| 10.0                    | 0.53   |                      |
| 11.0                    | 0.71   |                      |
| 12.0                    | 0.89   | 0.05                 |
| 13.0                    | 1.10   | 0.09                 |
| 14.0                    | 1.33   | 0.13                 |
| 15.0                    | 1.53   | 0.18                 |
| 16.0                    | 1.75   | 0.22                 |
| 17.0                    | 1.90   | 0.25                 |
| 18.0                    | 2.05   | 0.29                 |
| 19.0                    | 2.21   | 0.34                 |
| 20.0                    | 2.36   | 0.38                 |
| 22.0                    | 2.45   | 0.47                 |
| 24.0                    | 2.53   | 0.56                 |
| 26.0                    | 2.61   | 0.64                 |
| 28.0                    | 2.69   | 0.73                 |
| 30.0                    | 2.76   | 0.83                 |
| 35.0                    | 2.95   | 0.96                 |
| 40.0                    | 3.13   | 1.09                 |
| 45.0                    | 3.32   | 1.14                 |
| 50.0                    | 3.50   | 1.18                 |
| 60.0                    | 3.66   | 1.22                 |
| 70.0                    | 3.70   | 1.25                 |
| 80.0                    | 3.70   | 1.24                 |
| 90.0                    | 3.63   | 1.22                 |
| 100.0                   | 3.56   | 1.20                 |
| 120.0                   | 3.45   | 1.10                 |
| 140.0                   | 3.26   | 1.02                 |
| 160.0                   | 3.10   | 0.93                 |
| 180.0                   | 2.90   | 0.85                 |
| 200.0                   | 2.72   | 0.78                 |

In summary, four observations should be noted: (i) the parent ionization cross section for all three targets SiD<sub>x</sub> ( $x = 1-3$ ) has essentially the same maximum value of  $3.7 \times 10^{-16}$  cm<sup>2</sup> at 70 eV, (ii) for all three targets, parent ionization is the dominant process and the most prominent dissociative ionization channel is the one in which one D atom is removed, i.e., SiD<sub>x</sub> → SiD<sub>x-1</sub><sup>+</sup> + D, (iii) the cross section for the formation of the dominant fragment ion also has essentially the same value of about  $1.2 \times 10^{-16}$  cm<sup>2</sup> (at 70 eV) for all three targets, and (iv) the dominant fragment ions are formed with little excess kinetic energy.

There are some notable similarities between the present SiD<sub>x</sub> cross sections and the cross-section data obtained previously for CD<sub>x</sub> and SiF<sub>x</sub>.<sup>9-12</sup> Similar to what we found here, the ionization of the CD<sub>x</sub> radicals was also dominated by parent ionization and the parent ionization cross section had essentially the same value for all CD<sub>x</sub> targets. Furthermore, dissociative ionization of the CD<sub>x</sub> radicals was also dominated by a single channel which involved the removal of a D atom. However, the present SiD<sub>x</sub> cross sections are typically larger than the corresponding CD<sub>x</sub> cross sections by more

than a factor of 2. On the other hand, the previously measured SiF<sub>x</sub> ionization cross sections showed maximum values comparable to and in some cases even larger than the present SiD<sub>x</sub> cross sections. However, dissociative ionization channels were found to be much more important for SiF<sub>x</sub> than for SiD<sub>x</sub>. The presence of strong dissociative ionization channels appear to be characteristic for all fluorine-bearing molecules and radicals.<sup>16,20,24,26</sup>

## B. Total single ionization cross sections and comparison with calculations

Figures 5(a)–5(c) show a comparison between the calculated total single ionization cross section for SiH<sub>x</sub> ( $x = 1-3$ ) and the experimentally determined single ionization cross section for SiD<sub>x</sub> derived from the present data. In all cases, the experimental SiD<sub>x</sub> cross section was determined by summing the measured partial ionization cross sections, SiD<sub>3</sub><sup>+</sup> + SiD<sub>2</sub><sup>+</sup> for SiD<sub>3</sub>, SiD<sub>2</sub><sup>+</sup> + SiD<sup>+</sup> for SiD<sub>2</sub>, and SiD<sup>+</sup> + Si<sup>+</sup> for SiD. No allowance was made for the unobserved channels or for channels with peak cross sections of  $0.1 \times 10^{-16}$  cm<sup>2</sup> or less. Therefore, these cross section values represent lower limits of the experimental total single ionization cross sections. The calculated total single ionization cross sections were obtained from a modified additivity rule<sup>16</sup> which incorporates weighting factors in order to account for molecular bonding. The level of agreement between experimentally determined and calculated cross section is generally good to satisfactory. The experimental total single ionization cross section for all three targets is essentially the same with a maximum value of about  $5 \times 10^{-16}$  cm<sup>2</sup> at 70 eV. All calculated cross sections reach their maximum at a somewhat lower energy around 50 eV and decline more rapidly towards higher impact energies compared to the experimental cross sections. This behavior has also been observed before in the case of the SO, CD<sub>x</sub>, CF<sub>x</sub> and NF<sub>x</sub> radicals.<sup>12,15,25</sup>

The level of agreement between the experimentally determined maximum cross sections and the calculated maximum cross sections is best for SiD<sub>3</sub> with a 10% discrepancy. The agreement gets somewhat poorer for the simpler radicals with a 15% discrepancy for SiD<sub>2</sub> and a 30% discrepancy for SiD for the maximum ionization cross-section values. At 70 eV, the discrepancy between the calculated and the measured total single ionization cross section is about 5% for SiD<sub>3</sub> and SiD<sub>2</sub>, but rises to about 20% for SiD. A possible explanation for the larger discrepancy in the case of SiD could be the omission of the D<sup>+</sup>/SiD cross section (which was not measured) from the experimentally determined cross section. This omission can be expected to have the largest impact on the cross section for simplest target, SiD. Support for this assumption comes from the fact that a similar situation was observed in our previous studies of CD<sub>x</sub> ( $x = 1-4$ ), in which the level of agreement between measured and calculated total single ionization cross section was poorest for the CD radical, and by the fact that an earlier study of the ionization of the SiF<sub>x</sub> radicals<sup>9-11</sup> revealed the largest partial cross section of the F<sup>+</sup> fragment ion for the SiF parent radical.

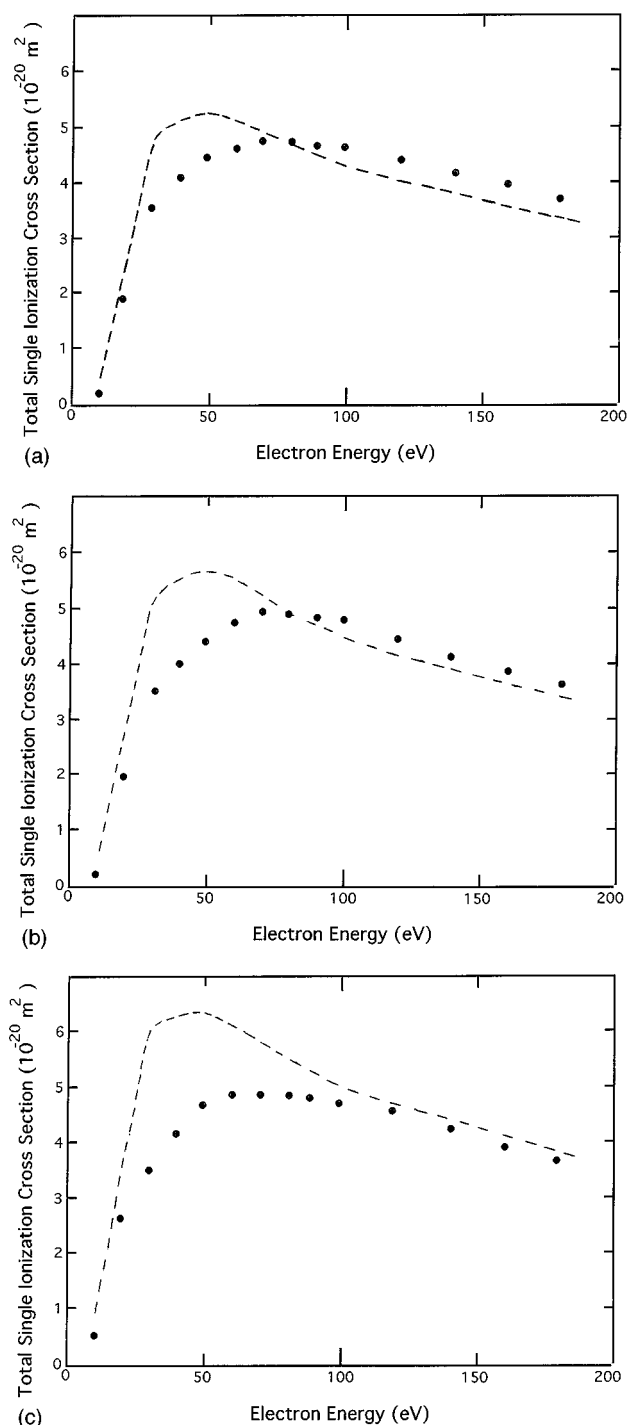


FIG. 5. Experimental (●) and calculated (--) total single ionization cross sections as a function of electron energy, (a)  $\text{SiD}_3$ , (b)  $\text{SiD}_2$ , and (c)  $\text{SiD}$ . (See text for further details.)

#### IV. SUMMARY

The fast-beam technique has been used in a series of measurements of the electron-impact ionization and dissociative ionization of the  $\text{SiD}_x$  ( $x=1-3$ ) free radicals for impact energies up to 200 eV. The most noteworthy findings are (i) a parent ionization cross section for all three targets  $\text{SiD}_x$  ( $x=1-3$ ) which has essentially the same maximum value of

about  $3.7 \times 10^{-16} \text{ cm}^2$ , (ii) a dominance of parent ionization vs dissociative ionization, (iii) the existence of a single prominent dissociative ionization channel for all three targets, viz. the one in which one D atom is removed, and (iv) a cross section for this dominant dissociative ionization channel which has essentially the same maximum value for all three targets, about  $1.2 \times 10^{-16} \text{ cm}^2$ . A comparison of the experimentally determined total (single) ionization cross sections with calculated cross sections based on a recently introduced modified additivity rule showed good to satisfactory agreement for all three targets.

#### ACKNOWLEDGMENTS

This work was supported by the Division of Chemical Sciences, Office of Basic Energy Sciences, Office of Energy Research, U.S. Department of Energy. We also acknowledge the U.S. National Aeronautics and Space Administration (NASA Grant NAGW-4118) for partial support of the research equipment used in the present work and for partial support for one of us (V.T.) in the early stages of this work. We are also grateful for travel support from a NATO Collaborative Research Grant (CRG-920089). The authors wish to thank Professor T. D. Märk, Dr. R. Basner, and Dr. M. Schmidt for many helpful discussions. We also thank Mr. Alexander Levin for his assistance in the early phase of the data acquisition.

- <sup>1</sup>T. Glenewinkel-Meyer, J. A. Bartz, G. M. Thorson, and F. F. Crim, *J. Chem. Phys.* **99**, 5944 (1993), and references therein to earlier work.
- <sup>2</sup>P. Fons, T. Motooka, K. Awazu, and H. Onuki, *Appl. Surf. Science* **79/80**, 476 (1994).
- <sup>3</sup>K. Tonokura, Y. Mo, Y. Matsumi, and M. Kawasaki, *J. Chem. Phys.* **96**, 6688 (1992).
- <sup>4</sup>F. E. Saalfeld and H. J. Svec, *Inorg. Chem.* **2**, 466 (1963).
- <sup>5</sup>P. Haaland, *Chem. Phys. Lett.* **170**, 146 (1990).
- <sup>6</sup>H. Chatham, D. Hils, R. Robertson, and A. Gallagher, *J. Chem. Phys.* **81**, 1770 (1984).
- <sup>7</sup>E. Krishnakumar and S. K. Srivastava, *Contr. Plasma Phys.* **35**, 395 (1995).
- <sup>8</sup>R. Basner and M. Schmidt (private communication); R. Basner, M. Schmidt, V. Tarnovsky, and K. Becker, *Int. J. Mass Spectrom. Ion Proc.* (to be published).
- <sup>9</sup>T. R. Hayes, R. C. Wetzel, F. A. Biaocchi, and R. S. Freund, *J. Chem. Phys.* **88**, 823 (1989).
- <sup>10</sup>T. R. Hayes, R. J. Shul, F. A. Biaocchi, R. C. Wetzel, and R. S. Freund, *J. Chem. Phys.* **89**, 4035 (1989).
- <sup>11</sup>R. J. Shul, T. R. Hayes, R. C. Wetzel, F. A. Biaocchi, and R. S. Freund, *J. Chem. Phys.* **89**, 4042 (1989).
- <sup>12</sup>V. Tarnovsky, A. Levin, H. Deutsch, and K. Becker, *J. Phys. B* **29**, 139 (1996).
- <sup>13</sup>T. D. Märk and F. Egger, *J. Chem. Phys.* **67**, 2629 (1977).
- <sup>14</sup>T. D. Märk, F. Egger, and M. Cheret, *J. Chem. Phys.* **67**, 3795 (1977).
- <sup>15</sup>R. Basner, M. Schmidt, H. Deutsch, V. Tarnovsky, A. Levin, and K. Becker, *J. Chem. Phys.* **103**, 211 (1995).
- <sup>16</sup>H. Deutsch, T. D. Märk, V. Tarnovsky, K. Becker, C. Cornelissen, L. Cespiva, and V. Bonacic-Koutecky, 1994 *Int. J. Mass Spectrom. Ion Proc.* **137**, 77 (1994).
- <sup>17</sup>R. C. Wetzel, F. A. Biaocchi, T. R. Hayes, and R. S. Freund, *Phys. Rev. A* **35**, 559 (1987).
- <sup>18</sup>R. S. Freund, R. C. Wetzel, R. J. Shul, and T. R. Hayes, *Phys. Rev. A* **41**, 3575 (1990).
- <sup>19</sup>V. Tarnovsky and K. Becker, *Z. Phys. D* **22**, 603 (1992).
- <sup>20</sup>V. Tarnovsky and K. Becker, *J. Chem. Phys.* **98**, 7868 (1993).
- <sup>21</sup>S. G. Lias, J. E. Bartmess, J. F. Liebman, J. L. Holmes, R. D. Levine, and W. G. Mallard, *J. Phys. Chem. Ref. Data* **17**, 1 (1988).

- <sup>22</sup>D. D. Wagman, W. H. Evans, V. B. Parker, R. H. Schumm, I. Halow, S. M. Bailey, K. L. Churney, and R. L. Nuttall, *J. Phys. Chem. Ref. Data* **11**, 1 (1982).
- <sup>23</sup>M. W. Chase, Jr., K. A. Davis, J. R. Downey, D. J. Frurip, R. A. McDonald, and A. N. Syverud, *J. Phys. Chem. Ref. Data* **14**, 1 (1985).
- <sup>24</sup>V. Tarnovsky, P. Kurunczi, D. Rogozhnikov, and K. Becker, *Int. J. Mass Spectrom. Ion Proc.* **128**, 181 (1993).
- <sup>25</sup>V. Tarnovsky, A. Levin, and K. Becker, *J. Chem. Phys.* **102**, 770 (1995).
- <sup>26</sup>V. Tarnovsky, A. Levin, and K. Becker, *J. Chem. Phys.* **100**, 5626 (1994).
- <sup>27</sup>R. Robertson, D. Hils, H. Chatham, and A. Gallagher, *Appl. Phys. Lett.* **43**, 544 (1993).
- <sup>28</sup>G. Herzberg, *Molecular Spectra and Molecular Structure* (Van Nostrand-Reinhold, New York, 1950), Vols. I and III.
- <sup>29</sup>*The Handbook of Chemistry and Physics*, 65th ed., edited by R. C. Weast, M. J. Astle, and W. H. Beyer (CRC, Boca Raton, 1985).